BLIND CYCLOSTATIONARY STATISTICS BASED CARRIER FREQUENCY OFFSET AND SYMBOL TIMING DELAY ESTIMATORS IN FLAT-FADING CHANNELS

Y. Wang[1], E. Serpedin[1], P. Ciblat[2] and P. Loubaton[3]

[1] Dept. of Electrical Engineering, Texas A&M University, College Station, TX 77843, USA
[2] Ecole Nationale Supérieure des Télécommunications, Paris, France
[3] Université de Marne-la-Vallée, Lab. "Systèmes de Communication", Marne-la-Vallée, France

ABSTRACT

Blind carrier frequency offset and symbol timing delay estimators for linearly modulated waveforms transmitted through flat-fading channels have been recently developed by exploiting the received signal's second-order cyclostationary statistics in [2], [3], and [6]. The goal of this paper is to establish and analyze the asymptotic (large sample) performance of the estimators [2] and [3], as a function of the pulse shape bandwidth and the oversampling factor. It is shown that the performance of these estimators improves as the pulse shape bandwidth increases and by selecting small values for the oversampling factor.

INTRODUCTION

In digital communication systems, the re-acquisition of synchronization must often be performed in a fast and reliable way without sacrificing bandwidth for periodic re-training. Therefore, developing optimal non-data aided (or blind) synchronization architectures appears as an important problem. Recently, blind carrier frequency offset and symbol timing delay estimators that exploit the second-order cyclostationary (CS) statistics, introduced by oversampling the continuous-time received waveform at a rate faster than Nyquist rate have been proposed in [2], [3], and [6].

The goal of this paper is to analyze and design criteria for improving the performance of the feedforward non-data aided carrier frequency offset and symbol timing delay estimators [2] and [3] with respect to (w.r.t.) the pulse shape bandwidth and oversampling factor. The theoretical asymptotic (large sample) performance of the Gini-Giannakis (GG) [3] and Ghogho-Swami-Durrani (GSD) [2] estimators is established, and it is shown that the performance of these estimators improves by selecting a small value for the oversampling factor ($P = 3$) and pulse shapes with larger bandwidths. By properly taking into account the aliasing effects, it is shown that the symbol timing delay estimates corresponding to the GG and GSD estimators take a slightly different form than the expressions reported in [2] and [3] in the case when $P = 2$.

MODELING ASSUMPTIONS

Consider the baseband representation of a linearly modulated signal transmitted through a flat-fading channel. The receiver output can be expressed as[1] (see e.g., [2] and [3]):

$$x_c(t) = \mu_c(t) e^{j2\pi f_e t} \sum_l w(l) h_c(t - \epsilon T - lT) + v_c(t) \ , \quad (1)$$

where $\mu_c(t)$ is the fading-induced noise, $w(l)$'s are independently and identically distributed (i.i.d.) input symbols, $h_c(t)$ denotes the convolution of the transmitter's signaling pulse and the receiver filter, $v_c(t)$ is the complex-valued additive noise, T is the symbol period, f_e and ϵ stand for carrier frequency offset and symbol timing delay, respectively, and represent the parameters to be estimated.

By oversampling the received signal $x_c(t)$ (see eq. (1)) with the sampling period $T_s := T/P$ ($P \geq 2$), the following discrete-time channel model is obtained:

$$x(n) = \mu(n) e^{j2\pi f_e T n/P} \sum_l w(l) h(n - lP) + v(n) \ , \quad (2)$$

with[2] $x(n) := x_c(nT_s)$, $\mu(n) := \mu_c(nT_s)$, $v(n) := v_c(nT_s)$, and $h(n) := h_c(nT_s - \epsilon T)$. In order to simplify the derivation of the asymptotic performance of estimators [2], [3], we assume the following:

(**AS1**) $w(n)$ is a zero-mean i.i.d. sequence with $\sigma_w^2 = 1$.

(**AS2**) $\mu(n)$ is a constant noise with unit energy. Later

[1] The subscript $_c$ is used to denote a continuous-time signal.

[2] The notation := stands for *is defined as*.

0-7803-7225-5/01/$17.00 (c) 2001 IEEE

on, this assumption will be relaxed by considering that $\mu(n)$ is a time-selective fading process.

(**AS3**) $v(n)$ is a complex-valued zero-mean white process independent of $w(n)$, with variance σ_v^2.

(**AS4**) the combined filter $h_c(t)$ is a raised cosine pulse of bandwidth $[-(1+\rho)/2T, (1+\rho)/2T]$, where the roll-off factor ρ satisfies $(0 \le \rho < 1)$ [4, Ch. 9].

(**AS5**) frequency offset f_e is small enough so that the mismatch of the receive filter due to f_e can be neglected [3]. Generally, the condition $f_e T < 0.2$ is assumed.

BLIND CARRIER FREQUENCY OFFSET AND TIMING DELAY ESTIMATORS

In this paper, the time-varying correlation of $x(n)$ is defined as $c_{2x}(n;\tau) := E\{x^*(n)x(n+\tau)\}$, where τ is an integer lag. Based on the eq. (2), straightforward calculations lead to the following relation: $c_{2x}(n;\tau) = c_{2x}(n+P;\tau)$, $\forall n, \tau$. Being periodic, $c_{2x}(n;\tau)$ admits a Fourier Series (FS) expansion whose FS-coefficients, termed cyclic correlations, are given by the following expression according to Eq. (2):

$$C_{2x}(k;\tau) = \frac{\sigma_w^2}{P} e^{j2\pi \frac{f_e T \tau}{P}} \left(\sum_n h^*(n) h(n+\tau) e^{-j2\pi \frac{kn}{P}} \right) + \sigma_v^2 \delta(\tau)\delta(k) \ , \tag{3}$$

where $\delta(.)$ stands for the Kronecker's delta. Based on the Parseval's relation, an alternative expression for $C_{2x}(k;\tau)$ is next derived when $P \ge 3$ [2], [3]:

$$C_{2x}(k;\tau) = \frac{\sigma_w^2}{P} e^{j2\pi f_e T\tau/P} e^{-j2\pi k \epsilon} G_2(k;\tau) e^{j\pi k\tau/P} + \sigma_v^2 \delta(\tau)\delta(k), \tag{4}$$

where:

$$G_2(k;\tau) := \frac{P}{T} \int_{-\frac{P}{2T}}^{\frac{P}{2T}} H_c(F - \frac{k}{2T}) H_c(F + \frac{k}{2T}) e^{j2\pi F\tau T/P} dF.$$

In the case when $P = 2$, the aliasing effects due to frequency-shifting can not be avoided. By properly taking into account the aliasing effects, one can show that for $P = 2$ the following eq. holds:

$$C_{2x}(1;\tau) = \frac{2\sigma_w^2}{P} e^{j2\pi f_e T\tau/P} \cos\left[2\pi \left(\epsilon + \frac{\tau}{4}\right)\right] \cdot G_3(1;\tau) e^{j2\pi\tau/P} \ , \tag{5}$$

where:

$$G_3(k;\tau) := \frac{2}{T} \int_{-\frac{1}{2T}}^{\frac{1}{2T}} H_c(F - \frac{k}{2T}) H_c(F + \frac{k}{2T}) e^{j2\pi F\tau T/P} dF.$$

Due to the symmetry properties of the raised-cosine function $h_c(t)$, it is easy to check that $G_2(k;\tau)$ and $G_3(k;\tau)$ are real-valued functions and non-zero only for cycles $k = 0, \pm 1$. Furthermore, from these cyclic correlations, it is usual to define a cyclic spectrum for each cyclic frequency k, as follows:

$$S_{2x}(k;f) := \sum_\tau C_{2x}(k;\tau) e^{-j2\pi\tau f}.$$

We also define the conjugated second-order time-varying correlation of $x(n)$ as

$$\widetilde{c}_{2x}(n;\tau) := \mathrm{E}\{x(n)x(n+\tau)\}.$$

It is easy to check that $\widetilde{c}_{2x}(n;\tau)$ can be expressed as

$$\widetilde{c}_{2x}(n;\tau) = \sum_{k=0}^{P-1} \widetilde{C}_{2x}(k;\tau) e^{j2\pi \frac{(k+2f_e T)n}{P}} \ ,$$

where

$$\widetilde{C}_{2x}(k,\tau) = \frac{\sigma_{c,w}^2}{P} e^{j2\pi \frac{f_e T\tau}{P}} \left(\sum_n h(n) h(n+\tau) e^{-j2\pi \frac{kn}{P}} \right) \ ,$$

with $\sigma_{c,w}^2 := E\{w^2(n)\}$. In a similar way, we can define the conjugated cyclic spectrum $\tilde{S}_{2x}(k;f)$ as the Fourier transform (FT) of the sequence $\{\widetilde{C}_{2x}(k;\tau)\}_\tau$.

In practice, the cyclic correlations $C_{2x}(k;\tau)$ have to be estimated from a finite number of samples N. The standard sample estimate of C_{2x} is given by (see e.g., [1] and [3]):

$$\hat{C}_{2x}(k;\tau) = \frac{1}{N} \sum_{n=0}^{N-\tau-1} x^*(n) x(n+\tau) e^{-j2\pi kn/P} \ , \ \tau \ge 0 \ .$$

Relying on the eqs. (4 and 5), we can obtain the following estimators for the frequency offset f_e and the timing delay ϵ:

$$\hat{f}_e = \frac{P}{4\pi T\tau} \arg\{\hat{C}_{2x}(1;\tau)\hat{C}_{2x}(-1;\tau)\} \ , \tag{6}$$

$$\hat{\epsilon} = -\frac{1}{2\pi} \arg\{\hat{C}_{2x}(1;\tau) e^{-\frac{j\pi\tau(2f_e T+1)}{P}}\}, \ P \ge 3, \tag{7}$$

$$\hat{\epsilon} = \frac{1}{2\pi} \arccos\left\{\mathrm{re}\Big(\frac{\hat{C}_{2x}(1;\tau) e^{-j\pi\tau(\hat{f}_e T+1)}}{\sigma_w^2 G_3(1;\tau)}\Big)\right\} - \frac{\tau}{4} \ , \quad P = 2 \ . \tag{8}$$

As described in [2], the performance of the frequency offset and timing delay estimators does not change significantly with τ. In this paper, we choose $\tau = 1$ for the GG estimator. One can see that in this case, the frequency offset estimators corresponding to the GSD [2, eq. (7)] and GG [3, eq. (10)] algorithms coincide. However, in the case of the timing delay estimators corresponding to the GSD algorithm, τ is set to 0.

PERFORMANCE ANALYSIS

The estimators of f_e and ϵ are asymptotically unbiased and consistent [2], [3]. In this section, we will establish the asymptotic variances of $\hat{f}_e$ and $\hat{\epsilon}$, which are defined as

$$\gamma_{f_e} := \lim_{N\to\infty} N\mathrm{E}\{(\hat{f}_e - f_e)^2\}\ , \gamma_\epsilon := \lim_{N\to\infty} N\mathrm{E}\{(\hat{\epsilon} - \epsilon)^2\}\ , \quad (9)$$

respectively. If we define the normalized unconjugated and conjugated asymptotic variances of the cyclic correlations by means of the following relations [1]:

$$\left[\boldsymbol{\Gamma}^{(k,m)}\right]_{u,v} := \lim_{N\to\infty} N\mathrm{E}\Big\{\Big(\hat{C}_{2x}(k,u) - C_{2x}(k,u)\Big) \cdot \Big(\hat{C}_{2x}(m,v) - C_{2x}(m,v)\Big)^*\Big\}\ ,$$

$$\left[\widetilde{\boldsymbol{\Gamma}}^{(k,m)}\right]_{u,v} := \lim_{N\to\infty} N\mathrm{E}\Big\{\Big(\hat{C}_{2x}(k,u) - C_{2x}(k,u)\Big) \cdot \Big(\hat{C}_{2x}(m,v) - C_{2x}(m,v)\Big)\Big\}\ ,$$

where $k,\ m = \pm 1$, then the following proposition, which is an extension of the result presented in [1], can be established:

Proposition 1. *The asymptotic variances of the cyclic correlations are given by:*

$$\boldsymbol{\Gamma}^{(1,1)}_{u,v} = \sum_{k=0}^{P-1} e^{j2\pi\frac{kv}{P}} \int_0^1 S_{2x}(k;f) S^*_{2x}(k;f-\frac{1}{P}) e^{j2\pi(u-v)f} df + \sum_{k=0}^{P-1} e^{-j2\pi\frac{(1+k+2f_eT)v}{P}} \int_0^1 \tilde{S}_{2x}(k;f) \tilde{S}^*_{2x}(k;f-\frac{1}{P}) e^{j2\pi(u+v)f} df + \kappa P Q(P) C_{2x}(1;u) C^*_{2x}(1;v)\ ,$$

$$\boldsymbol{\Gamma}^{(1,-1)}_{u,v} = \sum_{k=0}^{P-1} e^{j2\pi\frac{kv}{P}} \int_0^1 S_{2x}(k;f) S^*_{2x}(k-2;f-\frac{1}{P}) e^{j2\pi(u-v)f} df + \sum_{k=0}^{P-1} e^{j2\pi\frac{(1-k-2f_eT)v}{P}} \int_0^1 \tilde{S}_{2x}(k;f) \tilde{S}^*_{2x}(k-2;f-\frac{1}{P}) e^{j2\pi(u+v)f} df + \kappa P C_{2x}(1;u) C^*_{2x}(-1;v)\ ,$$

$$\boldsymbol{\Gamma}^{(-1,1)}_{u,v} = \boldsymbol{\Gamma}^{*(1,-1)}_{v,u}\ , \quad \boldsymbol{\Gamma}^{(-1,-1)}_{u,v} = e^{j2\pi\frac{(v-u)}{P}} \boldsymbol{\Gamma}^{(1,1)}_{-v,-u}\ ,$$

and κ denotes the kurtosis of $w(n)$, $Q(P) = 1$ for $P \geq 3$ and $Q(P) = 2$ for $P = 2$.

In the above proposition, some terms within the sums may cancel out. Indeed, since the filter $h_c(t)$ is band-limited, the cyclic spectra at cycles $|k| > 1$ are zero. This remark implies, for example, that if $P > 4$, then only the terms driven by the index $k = 0$ remain in the expression of $\boldsymbol{\Gamma}^{(1,1)}$ and $k = 1$ in $\boldsymbol{\Gamma}^{(1,-1)}$. When $P = 2$, only $\boldsymbol{\Gamma}^{(1,1)}$ is needed since $C_{2x}(1;\tau) = C_{2x}(-1;\tau)$.
Since $C_{2x}(k;\tau) = e^{j2\pi k\tau/P} C^*_{2x}(-k;-\tau)$, it follows also that:

$$\left[\widetilde{\boldsymbol{\Gamma}}^{(k,m)}\right]_{u,v} = e^{j2\pi mv/P} \left[\boldsymbol{\Gamma}^{(k,-m)}\right]_{u,-v}\ .$$

By exploiting Proposition 1 and the eqs. (6), (7) and (8), the asymptotic variances of $\hat{f}_e$ and $\hat{\epsilon}$ for GG and GSD estimators can be obtained and are given by[3]:

Proposition 2. *The asymptotic variance of the GG and GSD frequency offset estimators for $P \geq 3$ is given by:*

$$\gamma_{f_e} = \frac{P^4\left(\boldsymbol{\Psi}^T\boldsymbol{\Gamma}\boldsymbol{\Psi}^* - \mathrm{re}\{e^{-j4\pi f_eT/P}\boldsymbol{\Psi}^T\tilde{\boldsymbol{\Gamma}}\boldsymbol{\Psi}\}\right)}{32\pi^2T^2\sigma_w^4G_2^2(1;1)}$$

where

$$\boldsymbol{\Psi} = [\psi,\ \psi^*]^T\ , \quad \psi = e^{j2\pi(\epsilon-1/2P)}\ ,$$

$$\boldsymbol{\Gamma} = \begin{bmatrix} \boldsymbol{\Gamma}^{(1,1)}_{1,1} & \boldsymbol{\Gamma}^{(1,-1)}_{1,1} \\ \boldsymbol{\Gamma}^{(-1,1)}_{1,1} & \boldsymbol{\Gamma}^{(-1,-1)}_{1,1} \end{bmatrix},$$

and $\tilde{\boldsymbol{\Gamma}}$ is defined in a similar way as $\boldsymbol{\Gamma}$.
For $P = 2$, the asymptotic variance takes the expression:

$$\gamma_{f_e} = \frac{\mathbf{1}^T\boldsymbol{\Gamma}\mathbf{1} - \mathrm{re}\{e^{-j2\pi f_eT}\mathbf{1}^T\tilde{\boldsymbol{\Gamma}}\mathbf{1}\}}{8\pi^2T^2\sigma_w^4\sin^2(2\pi\epsilon)G_3^2(1;1)},$$

with $\mathbf{1} = [1,1]^T$.

Proposition 3. *The asymptotic variance of the GG timing delay estimator for $P \geq 3$ is given by:*

$$\gamma_\epsilon = \frac{P^2\mathrm{re}\{e^{-j4\pi f_eT/P}\tilde{\boldsymbol{\Gamma}}^{(1,-1)}_{1,1} - \psi^2\boldsymbol{\Gamma}^{(1,-1)}_{1,1}\}}{8\pi^2\sigma_w^4G_2^2(1;1)} + \frac{T^2}{P^2}\gamma_{f_e}\ .$$

For $P = 2$, the asymptotic variance takes the expression:

$$\gamma_\epsilon = \frac{\boldsymbol{\Gamma}^{(1,1)}_{1,1} + \mathrm{re}\{e^{-j2\pi f_eT}\tilde{\boldsymbol{\Gamma}}^{(1,1)}_{1,1}\}}{8\pi^2\sigma_w^4\cos^2(2\pi\epsilon)G_3^2(1;1)}.$$

Proposition 4. *The asymptotic variance of the GSD timing delay estimator for $P \geq 3$ is given by:*

$$\gamma_\epsilon = \frac{P^2\left(\boldsymbol{\Gamma}^{(1,1)}_{0,0} - \mathrm{re}\{e^{j4\pi\epsilon}\tilde{\boldsymbol{\Gamma}}^{(1,1)}_{0,0}\}\right)}{8\pi^2\sigma_w^4G_2^2(1;0)}.$$

For $P = 2$, the asymptotic variance takes the form:

$$\gamma_\epsilon = \frac{\boldsymbol{\Gamma}^{(1,1)}_{0,0} + \mathrm{re}\{\tilde{\boldsymbol{\Gamma}}^{(1,1)}_{0,0}\}}{8\pi^2\sigma_w^4\sin^2(2\pi\epsilon)G_3^2(1;0)}\ .$$

EXTENSION TO TIME-SELECTIVE CHANNELS

Due to the assumption (**AS2**), the foregoing discussion applies only to time-invariant channels. In this section, we will see that the results obtained in the last section can be extended to the case of time-selective fading

[3] "re" and "im" stand for the real and imaginary part, respectively.

effects as long as the fading distortion $\mu_c(t)$ is approximately constant over a pulse duration or, equivalently, the Doppler spread $B_\mu T$ is small, where B_μ denotes the bandwidth of $\mu_c(t)$ [3].

Assuming now that $\mu(n)$ is a stationary complex process with autocorrelation $r_\mu(\tau) := \mathrm{E}\{\mu^*(n)\mu(n+\tau)\}$ [3], we can rewrite Eq. (3) for $k = \pm 1$ as:

$$C_{2x}(k;\tau) = \frac{\sigma_w^2}{P} r_\mu(\tau) e^{j2\pi \frac{f_e T \tau}{P}} \sum_n h^*(n)h(n+\tau)e^{-j2\pi \frac{kn}{P}} \ . \quad (10)$$

Based on Eq. (10), it is not difficult to find that all the previous estimators (Eqs. (6)–(8)) still hold true except that for $P = 2$ they take the form:

$$\hat{\epsilon} = \frac{1}{2\pi} \arccos \Big\{ \mathrm{re}\Big(\frac{\hat{C}_{2x}(1;1)e^{-j\pi(\hat{f}_e T+1)}}{\sigma_w^2 G_3(1;1) r_\mu(1)} \Big) \Big\} - \frac{1}{4} \ ,$$
$$\hat{\epsilon} = \frac{1}{2\pi} \arccos \Big\{ \mathrm{re}\Big(\frac{\hat{C}_{2x}(1;0)}{\sigma_w^2 G_3(1;0) r_\mu(0)} \Big) \Big\} \ , \quad (11)$$

respectively.

Compared with the performance analysis reported in the last section, the exact asymptotic variance of GG and GSD estimators in the case of time-selective channels supports several modifications. Introduce now an additional assumption on the fading channel:
(**AS6**): the land-mobile channel is a Rayleigh fading channel, which means that $\mu(n)$ is a zero-mean complex-valued circular Gaussian process [4].

For general land-mobile channel models, the autocorrelation of $\mu(n)$ is proportional to the zero-order Bessel function, i.e., $r_\mu(\tau) \propto J_0(2\pi B_\mu \tau)$ (c.f. [5]). Based on the assumption (**AS6**), $\tilde{r}_x(n;\tau) = 0$ and the higher-order cumulants of $x(n)$ are also zero. Therefore, one can find that in the presence of time-selective fading effects, the performance analysis can be established in a similar way as in the case of time-invariant fading channels. In fact, considering the assumption (**AS6**), only the first terms of $\mathbf{\Gamma}_{u,v}^{(1,1)}$ and $\mathbf{\Gamma}_{u,v}^{(1,-1)}$ in Proposition 1 survive, and the asymptotic variances γ_{f_e} and γ_ϵ for the GG and GSD estimators in Propositions 2-4 still hold true except that some constants related to $r_\mu(1)$ or $r_\mu(0)$ should be added. For example, when $P = 2$, based on Eq. (11), we now obtain the following expressions for the asymptotic variances corresponding to the GG and GSD timing delay estimators:

$$\gamma_\epsilon = \frac{\mathbf{\Gamma}_{1,1}^{(1,1)} + \mathrm{re}\{e^{-j2\pi f_e T}\tilde{\mathbf{\Gamma}}_{1,1}^{(1,1)}\}}{8\pi^2\sigma_w^4 \cos^2(2\pi\epsilon) G_3^2(1;1) r_\mu^2(1)} \ ,$$
$$\gamma_\epsilon = \frac{\mathbf{\Gamma}_{0,0}^{(1,1)} + \mathrm{re}\{\tilde{\mathbf{\Gamma}}_{0,0}^{(1,1)}\}}{8\pi^2\sigma_w^4 \sin^2(2\pi\epsilon) G_3^2(1;0) r_\mu^2(0)} \ ,$$

respectively.

In closing this section, it is interesting to remark that for implementing the GG and GSD frequency-offset estimators no information regarding the time-varying fading process $\mu(n)$ is required. If the oversampling factor satisfies $P \geq 3$, then the implementation of the GG and GSD timing delay estimators does not require any knowledge of $\mu(n)$, too. However, when $P = 2$ knowledge of the second-order statistics $r_\mu(0)$ and $r_\mu(1)$ is required for implementing the GG and GSD timing delay estimators (11). However, simulation experiments, reported in the next section, show that from a computational complexity and performance viewpoint the best value of the oversampling factor is $P = 3$. Thus, estimation of parameters $r_\mu(0)$ and $r_\mu(1)$ can be avoided by selecting $P > 2$.

SIMULATIONS

In this section, the experimental Mean-Square Error (MSE) results and theoretical asymptotic bounds of estimators (6)-(8) are compared. The experimental results are obtained by performing a number of 400 Monte Carlo trials assuming that the transmitted symbols are i.i.d. linearly modulated symbols drawn from a QPSK constellation with $\sigma_w^2 = 1$. The number of symbols is set to $N = 200$ in all simulations. The transmit and receive filters are square-root raised cosine filters, and the continuous-time additive noise $v_c(t)$ is generated as Gaussian white noise with variance $\sigma_{v_c}^2$. The signal-to-noise ratio is defined as: SNR:= $10\log_{10}(\sigma_w^2/\sigma_{v_c}^2)$. Experiments 1 to 2 assume time-invariant channels corrupted by additive white discrete-time noise, and the parameters $f_e T = 0.011$ and $\epsilon T = 0.37$. To render the discrete-time noise uncorrelated, a front-end filter with two-sided bandwidth P/T is used [2]. Experiments 3 to 4 are performed assuming time-selective Rayleigh fading with $\epsilon T = 0.37$ and a larger frequency offset $f_e T = 0.2$, and the performance analysis of GG and GSD estimators is evaluated in the presence of additive colored discrete-time noise, i.e., when there is no front-end filter placed before the matched filter. In this scenario, for Experiments 3 and 4 the additive noise $v(n)$ is generated by passing $v_c(t)$ through the square-root raised cosine filter to yield a discrete-time noise with autocorrelation sequence $r_v(\tau) := \mathrm{E}\{v^*(n)v(n+\tau)\} = \sigma_{v_c}^2 h_c(\tau)$ [3]. In our simulations, the Doppler spread is set to $B_\mu T = 0.005$ (very slow fading), $\mu(n)$ is created by passing a unit-power zero-mean white Gaussian noise process through a normalized discrete-time filter, obtained by bilinearly transforming a third-order continuous-time all-pole filter, whose poles are the roots of the equation $(s^2+0.35\omega_0 s+\omega_0^2)(s+\omega_0)=0$, where $\omega_0=2\pi B_\mu/1.2$.

In all figures, the theoretical bounds of GG and GSD estimators are represented by the solid line and the dash line, respectively. The experimental results of GG and GSD estimators are plotted using dash-dot lines with stars and squares, respectively.

Experiment 1 : *Performance versus the oversampling rate P.* By varying the oversampling rate P, we compare the MSE of GG and GSD estimators with their theoretical asymptotic variances. The roll-off factor of the pulse shape is $\rho=0.5$, and SNR=20dB. The results are depicted in Figure 1.

Experiment 2 : *Performance versus the filter bandwidth.* Figure 2 depicts the MSE of the estimators versus the roll-off factor ρ assuming oversampling rate $P=4$ and SNR=20 dB.

Experiment 3 : *Performance versus the oversampling rate P in time-selective channels.* We repeat the Experiment 1 by assuming a time-selective channel corrupted by additive discrete-time colored noise. The roll-off factor of the pulse shape is $\rho=0.5$, and SNR=10dB. The results are depicted in Figure 3.

Experiment 4 : *Performance versus the filter bandwidth in time-selective channels.* Figure 4 depicts the MSE of the estimators versus the roll-off factor ρ in the presence of time-varying fading effects, assuming oversampling rate $P=4$ and SNR=10 dB.

Both experimental and theoretical results show that larger oversampling factors are not justifiable from a computational and performance analysis viewpoint. A smaller oversampling rate ($P=3$) and a wider pulse shape bandwidth ($\rho\in[0.6,\ 0.9]$) are preferred.

References

[1] P. Ciblat, P. Loubaton, E. Serpedin and G. B. Giannakis, "Asymptotic analysis of blind cyclic correlation based symbol-rate estimators," *IEEE Trans. Information Theory*, March 2000 (submitted).

[2] M. Ghogho, A. Swami and T. Durrani, "On blind carrier recovery in time-selective fading channels," *Asilomar*.

[3] F. Gini and G. B. Giannakis, "Frequency offset and symbol timing recovery in flat-fading channels," *IEEE Trans. Comm.*, March 1998.

[4] J. G. Proakis, *Digital Communications*, 1995.

[5] T. S. Rappaport, *Wireless Communications: Principles and Practice*, Prentice-Hall, 1996.

[6] K. E. Scott and E. B. Olasz, "Simultaneous clock phase and frequency offset estimation," *IEEE Trans. Comm.*, July 1995.

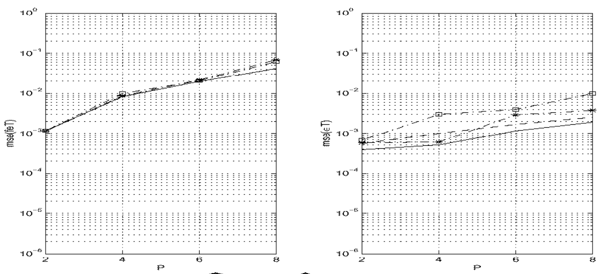

Figure 1: MSEs of $\widehat{f_e T}$ and $\widehat{\epsilon T}$ versus oversampling rate P.

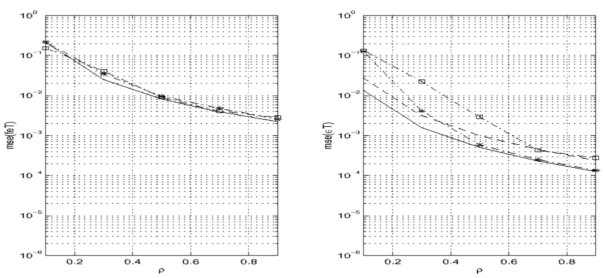

Figure 2: MSEs of $\widehat{f_e T}$ and $\widehat{\epsilon T}$ versus roll-off factor ρ.

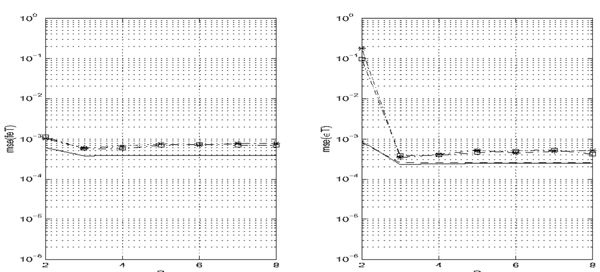

Figure 3: MSEs of $\widehat{f_e T}$ and $\widehat{\epsilon T}$ versus oversampling rate P in time-selective channels.

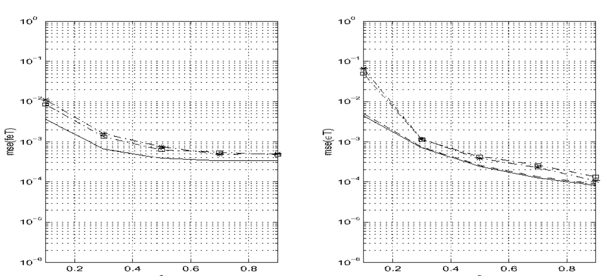

Figure 4: MSEs of $\widehat{f_e T}$ and $\widehat{\epsilon T}$ versus roll-off factor ρ in time-selective channels.